Available online at www.sciencedirect.com
SCIENCE DIRECT®
Journal of Power Sources 145 (2005) 161–168
JOURNAL OF POWER SOURCES
www.elsevier.com/locate/jpowsour

Characterisation of Co-based electrocatalytic materials for O_2 reduction in fuel cells

M. Manzoli *, F. Boccuzzi

Department of Inorganic, Physical and Materials Chemistry, NIS Centre of Excellence, University of Turin, via P. Giuria 7, 10125 Torino, Italy

Accepted 28 January 2005
Available online 26 April 2005

Abstract

Different cobalt containing materials obtained from the thermal decomposition of two organic precursors, cobalt–acetylacetonate and cobalt–tetrametoxyphenylporphyrin, and Co_3O_4 prepared by thermal decomposition of cobalt carbonate have been characterised by thermogravimetric analysis (TGA), X-ray diffraction (XRD) and high resolution transmission microscopy (HRTEM). It has been found that the cobalt precursor, the organic macrocycle and the active carbon are simultaneously needed during the heat treatment in inhert atmosphere. Their contemporaneous presence is useful to obtain a material on which the dispersed metal is able to catalyse reactions that produce pores or tunnels inside the carbon, thus resulting in an enhanced contact area. The organic macrocycle is only partially decomposed and the residual fraction could enhance the conductivity.

Keywords: Oxygen electroreduction; Cobalt precursors; Carbon black; TGA; HRTEM; XRD

1. Introduction

Oxygen reduction in gas diffusion electrodes attracts considerable interest primarily because of its impact on various energy-related fields, such as fuel cells and metal–air batteries. The cathode of the fuel cells, fed with umidified air, is usually made up of a carbon powder, mixed with a fluorined polymer, that works as an electrolyte, and then activated with a catalyst. Platinum has been traditionally employed as a catalyst for the oxygen reduction. Moreover, Pt and its alloys are usually used for hydrogen oxidation and also for oxygen reduction in the low temperature fuel cells [1,2]. Due to their high cost, less expensive alternatives, as for the oxygen reduction electrodes, have been actively searched for. One route is the use of transition metal macrocycles either unpyrolysed or pyrolysed. Carbon-supported metal macrocycles exhibit very good activity [3–5] and stability and are currently employed in mechanically recharged metal–air batteries for electrical traction [6,7]. However, their cost is quite high. Therefore, it is appealing to try to reproduce these electrocatalysts starting from different precursors of lower cost and easier availability, and to disclose the reasons for their activity to be able to improve their performance. Since the molecular structure of the catalyst is destroyed during the heat treatment, the metal complex is only a precursor of the actual active material [8–10]. In particular, it has been postulated that the nature of the catalytic site depends on the heat treatment temperature: metal–N_4 moieties (or their fragments) can be the active sites in the low and medium temperature range [11,12]. On the contrary, for catalysts prepared at high pyrolysis temperatures ($\geq$1123 K), where no metal–N bonds are detected anymore, metallic clusters surrounded by several layers of graphite are believed to be the catalytic centres [13]. However, the nature of the active sites produced at high temperature is still controversial. In a previous work [14], it has been shown that if cobalt–tetramethoxyphenylporphyrin (CoTMPP) is pyrolyzed at 1173 K with carbon black, a very

* Corresponding author. Tel.: +39 0116707541; fax: +39 0116707558.
E-mail address: maela.manzoli@unito.it (M. Manzoli).

0378-7753/$ – see front matter © 2005 Elsevier B.V. All rights reserved.
doi:10.1016/j.jpowsour.2005.01.062

active electrocatalyst results for the O_2 reduction in gas diffusion electrodes. A further analysis of the composition of the pyrolized material showed that some Co_3O_4 was present. Literature data report also that spinels of different oxides are active electrocatalysts in the oxygen reduction reaction [15,16]. Since these oxides are obtained by pyrolysis, as a first approach we have investigated the effect of the nature of the precursor on the activity of the Co_3O_4-based electrocatalysts. Moreover, literature works show that, to obtain an active electrocatalyst, the metal does not need to be incorporated in the macrocycle before pyrolysis. Thus, pyrolysis can be applied separately to a mixture of a metal salt and a macrocycle. Research work in this direction has been reported by Gupta et al. [17] and by Bouwkamp-Wijnoltz et al. [12]. More recently, Mocchi and Trasatti [18] compared the electrocatalytic activity of a pyrolysed mixture of CoTMPP and carbon black with those of composite electrocatalysts prepared by thermal decomposition of a cobalt oxide and a cobalt carbonate mixed with TMPP and carbon black. The authors found an appreciable increase in activity by using $CoCO_3$ and TMPP instead of the CoTMPP precursor in the carbon containing mixture and they hyphothesised a role of the presence carbon during the pyrolysis. It must be considered that oxygen reduction takes place in the three-zone interface, where the electron conducting material, the proton conducting electrolyte and the gas are in contact. Therefore, beside the nature of the employed materials, their interdispersion and the microstructure of the electrode are important, too. It has been shown that the life of the electrode mainly depends on the wetting properties of the porous mass. The electrochemical processes occur at the boundary between the micropores, that ensure the gas transportation, and the macropores, that contain the electrolyte. A bimodal pore size distribution of the porous mass of the carbon bonded PTFE is highly desired in order to optimize the electrodes behaviour [19,20]. The effects of different commercial carbon powders on the performance of gas diffusion electrodes were reported [7]. It was found that the catalytic activity and the physical characteristics of the carbon material strongly affect the performance and the life of the electrodes.

Here we present a characterisation by X-ray diffraction (XRD), thermogravimetric analysis (TGA) and high resolution transmission microscopy (HRTEM) of different cobalt-based catalysts in order to investigate the reasons of the different electrocatalytic activity exhibited by these systems.

2. Experimental

2.1. Materials

Commercial (Sigma–Aldrich) cobalt–tetramethoxyphenylporphyrin, Co(TMPP) ($C_{48}H_{36}CoN_4O_4$, 791.77 g mol^{-1}) and cobalt–acetylacetonate, $Co(acac)_3$, were employed as organic precursors of materials that can be potentially active in the activation of molecular O_2.

Two different carbon blacks, Vulcan XC72R obtained starting from furnace oil and produced by Cabot Corporation Ltd. and an acetylenic carbon, Shawinigan black AB50 produced by Chevron Chemical Co., have been chosen for this study. The chemico-physical properties of these carbon were provided by the manufacturers and they are reported in Table 1 together with the apparent density of the carbon treated with a fluorine resin (PTFE) reported in Ref. [7].

The lower wettability of the Shawinigan Black AB50 appears as a good pre-requisite in order to get larger three-phase-gas–solid–liquid interfaces.

Each carbon black was impregnated with a solution in acetone of the organic precursor to obtain the mixtures employed for the thermogravimetric analysis. The precursors content of the mixtures is different ($Co(acac)_3$, 4.71 wt.%; Co(TMPP), 10 wt.%) because of the different molecular weight of the organic ligand. The final Co content is 0.139 mmol g^{-1} for all the samples at the end of the preparation procedure (see also Table 2).

$CoCO_3$ and Co_3O_4 prepared by thermal decomposition at 673 K for 3 h of the same Co carbonate were also employed. Bare tetramethoxyphenylporphyrin, $C_{48}H_{38}N_4$ (Sigma–Aldrich) was introduced as additive during the thermal treatments of the mixtures containing these cobalt precursors and the carbon black. The following mechanical mixtures were prepared: $CoCO_3$ (10%) and Shawinigan Black AB50 (90%), $CoCO_3$ + TMPP, 10:1 ratio (10%) and Shawinigan Black AB50 (90%), Co_3O_4 (10%) and Shawinigan Black AB50 (90%), Co_3O_4 + TMPP, 10:1 ratio (10%) and Shawinigan Black AB50 (90%). The components were mechanically mixed in an agate mortar.

2.2. Methods

Thermogravimetric analysis (TGA) was carried out on a thermal analysis (TA) instrument (SDT 2960 model) by keep-

Table 1
Properties of the carbon blacks employed in this work

Sample	Source	Particles size (nm)	Surface area (m^2 g^{-1})	Total porosity (%)	C + PTFE 40% density (g cm^{-3})	Wet pore/total pore volume
Shawinigan Black AB50	Acetylene	40	82	47.3	0.15	0.17
Vulcan XC72R	Furnace oil	30	254	47.5	0.33	0.21

Table 2
Samples examined by TG analysis

Catalytic precursor	Carbon	Precursor/ carbon (wt.%)	mmol Co/g Carbon
CoTMPP	–	–	–
$Co(acac)_3$	–	–	–
–	Shawinigan AB50	–	–
–	Vulcan XC72R	–	–
Co(TMPP)	Vulcan XC72R	10	0.139
Co(TMPP)	Shawinigan AB50	10	0.139
$Co(acac)_3$	Shawinigan AB50	4.71	0.139

ing the samples under a constant flux of nitrogen, using a temperature ramp of 283 K min^{-1}, starting from room temperature (RT) up to 1273 K.

X-ray powder diffraction (XRD) patterns were obtained on a Philips PW1830 diffractometer using the Co Kα radiation (Kα = 1.7902 Å). The diffraction patterns were recorded at RT in the step scanning mode, with a 0.05° (2θ) step scan and 1 s $step^{-1}$ counting time in the range $10^\circ \leq 2\theta \leq 80^\circ$. The crystallite sizes were estimated by applying the Scherrer equation to all the peaks of the diffraction patterns.

High resolution transmission electron microscopy (HRTEM) measurements were made with a JEOL 2010 (200 kV) electron microscope, equipped with an EDS analytical system Oxford Link. The powders were ultrasonically dispersed in isopropyl alcohol and the suspension was deposited on a copper grid, coated with a porous carbon film. (The residual vacuum at the specimen region was approximately 1×10^{-6} mbar.) The size distributions of the particles were determined by considering at least 300 particles.

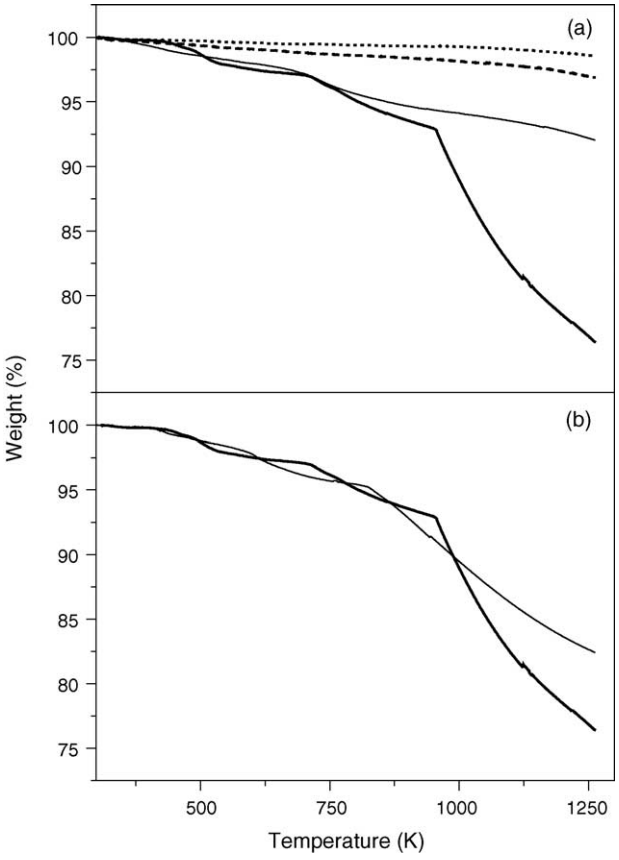

Fig. 1. Section a: TG curves of Shawinigan AB50 (dotted line), Vulcan XC72R (dashed line), Co(TMPP)/Shawinigan AB50 mixture (bold line) and Co(TMPP)/Vulcan XC72R mixture (fine line). Section b: comparison between the TG curves of $Co(acac)_3$/Shawinigan AB50 mixture (fine line) and CoTMPP/Shawinigan AB50 (bold line). The samples were kept under a constant flux of nitrogen, using a temperature ramp of 283 K min^{-1} and starting from RT up to 1273 K.

3. Results and discussion

The cathodic material, commonly fed with umidified air is constituted by a mixture of a carbon powder and a catalyst precursor, CoTMPP. This mixture is integrated in a body using perfluorosulfonic acid (PFSA) as proton conductor.

Since it is well known that both activity and stability of cobalt macrocycles are markedly enhanced if undergone to a thermal treatment, the mixture containing the carbon and the catalyst precursor is heat treated at 1173 K in a nitrogen atmosphere before the fabrication of the electrode.

A modification of the macrocyclic structure with the appearance of interactions with the carbon support occurs. Therefore, a thermogravimetric analysis performed on the carbon/precursor mixture can be very useful to have a deep insight on the processes occurring to the cathodic material during the thermal decomposition at high temperature.

The samples undergone to the heat treatment for the TGA analysis are summarized in Table 2. The bare carbon blacks and the precursors have been examined for comparison, too.

The weight losses % of the bare carbon blacks, Vulcan XC72R (dashed curve) and Shawinigan AB50 (dotted curve), of a mixture of Co(TMPP) with Vulcan XC72R (fine curve) and with Shawinigan AB50 (bold curve) recorded from RT up to 1273 K are reported in Fig. 1a. The gradual weight loss versus the temperature of the bare carbons is of very small entity. The change of the initial weight corresponds to 1.46% for Shawinigan (dotted curve) and to 2.83% for Vulcan (dashed curve). The TG profiles of the samples do not show any substantial change, being the little differences probably due to the desorption of water, initially present on the carbon surfaces, and of CO_2 molecules, that evolve from the desorption of carboxylic-like groups.

The total weight loss (22.53%) observed for the mixture containing Shawinigan AB50 impregnated with the Co(TMPP) precursor (bold curve) is bigger than the content of the organic precursor (10 wt.%). This trend is more evident starting from temperatures above 873 K. This phenomenon is not observed when Vulcan XC72R is employed (5.14%). Moreover, the excess of weight loss (16.16%) is less marked in the presence of the $Co(acac)_3$ precursor mix-

ture (see fine curve in Fig. 1b). These observations strongly indicate that the nature of the catalyst precursor and of the carbon black plays a decisive role during the preliminar heat treatment procedure.

We observed that in the presence of $Co(acac)_3$ (Fig. 1b, fine curve) and of CoTMPP (Fig. 1b, bold curve), the thermogravimetric profiles of Shawinigan AB50 are markedly changed if compared to that of the pure Shawinigan AB50 (see dotted curve in Fig. 1a). In both cases, similar processes involving carbon and induced by the cobalt species seem to take place in the presence of the organic precursor. In particular, the total weight loss observed for the mixture of carbon black and $Co(acac)_3$ is 15.89%. This value is higher respect to the precursor content (see Table 2). We also performed the TG analysis on the $Co(acac)_3$ precursor alone (not shown). It was found that the decomposition of this sample occurs in two steps in the temperature range between 488 and 513 K and two further steps in the range between 523 and 803 K. The total weight loss reaches the 89% and it mainly occurs in the first range of temperature. The cobalt content represents the 16.54% of the initial weight of the precursor, while the acetylacetonate ligand is calculated to be the 83.5%. The small excess observed in the total weight loss (89%) respect to this value can be ascribed to the desorption of water molecules. The $Co(acac)_3$ organic precursor is totally decomposed during the heat treatment in inert atmosphere. Keeping in mind these data, we can reasonably assume that the organic precursor is totally decomposed at 853 K. Differently from the bare precursor, the decomposition of the mixture takes place at higher temperatures (432 and 610 K).

The decomposition of the bare Co(TMPP) mainly takes place in two different steps: at 710 and 1018 K, as determined by the differential thermogravimetric minima of the signals (DTGA, data not shown). The total weight loss of Co(TMPP) is the 55.4% of the initial weight of the sample in the temperature range between RT and 1273 K. Cobalt represents the 7.4% of this value, while the porphyrin cycle is the 92.6%. The weight starts to decrease at about 633 K and it can be considered that the majority of this process occurs up to about 1000 K. The weight variation in this temperature range corresponds to the 42% of the sample and this value is markedly lower than the total weight calculated for the organic macrocycle (92.6%). This behaviour indicates that a residual fraction of the Co(TMPP) precursor is still present after the thermal treatment. Lalande et al. [21] explained the high electroactivity of heat treated cobalt phthalocyanine (CoPcTc) by the better conductivity of the polymeric material, or of its fragments, originated from the decomposition of the phthalocyanine. The enhanced conductivity would facilitate the O_2 reduction. A similar phenomenon probably occurs also for CoTMPP, since the TG measurements confirm a partial decomposition of the organic macrocycle.

The Shawinigan AB50 employed in our experiments is a carbon black of acetylenic provenience. Residual acetylenic fragments can transform into gaseous species at increasing temperatures. Quadrupole mass measurements reveal the presence of H_2 and C_2H_2 in the gas phase at temperatures over to 923 K (not shown for the sake of brevity). It has been reported that the VIII Group metals are very good catalysts for carbon gasification [22]. The metal catalysed gasification of carbon represents a very peculiar situation, since the carbon acts both as the support of the active phase, and as a reactant. The behaviour of this system is particular sensitive to eventual metal-support interactions. It is well known that the gasification of carbon catalysed by some transition metals (such as Ni, Ru, Rh and Os) occurs in two temperature regions, whatever the nature of the gasifying agent [23]: a low temperature region, between 673 and 973 K, the catalyst being severely deactivated between 873 and 973 K [24] and a high temperature region, above 1023 K, where the reaction occurs until all carbon is gasified. Calcium compounds are also used as catalysts of the gasification reaction to develop a mesoporous network in the carbon materials [25]. Some authors have reported that the metallic catalyst moves isotropically inside the active carbon to keep the contact with the carbon when it gasifies [26]. This phenomenon is called "tunneling". The eventual formation of tunnels inside the CoTMPP/Shawinigan mixture can produce an enhancement of the surface area and can explain the major electrocatalytic activity that we previously reported for this system [14].

Moreover, Alvim Ferraz et al. [27] compared different activated carbon impregnated with CoO, Co_3O_4 and CrO_3 in relation with the carbon structure, the catalyst content and the catalyst species. Two series of impregnated active carbons were prepared, the former by impregnation after activation, the latter by impregnation before activation. The authors found that, when compared with non-impregnated active carbons, the impregnated ones showed even a more significant contribution of micro- and mesoporosity. They explained their results by the presence of metallic species during the activation step, which by acting as catalyst, allowed the formation of a porous structure resulting in a greater total area and large pore volumes. The development of larger micro- and mesopores was more pronounced when the activation step was catalysed by Co_3O_4. Such a phenomenon may be at the origin of the enhanced catalytic activity of our system.

The XRD patterns of the Co(TMPP) precursor, of the Co(TMPP)/Shawinigan AB50 mixture and of the bare Shawinigan AB50 recorded after the heat treatment under nitrogen flux are reported in Fig. 2. We performed the XRD analysis in order to have information on the nature of the phases formed by the heat treatment.

The XRD pattern of the ex-Co(TMPP) precursor (dotted curve) contains peaks related to the CoO phase [$2\theta = 49.6^\circ$ and 72.95°; ICPDS file number 9-402] and to a cubic metallic Co phase [$2\theta = 51.75^\circ$ and 60.5°; JCPDS file number 15-806]. Moreover, the ex-CoTMPP sample exhibits peaks centred at $2\theta = 21.9^\circ$, 36.35°, 42.95°, 44.95°, 65.65°, 70.1° and 77.5°. These peaks are due to the presence of a Co_3O_4 cubic phase (JCPDS file number 9-418).

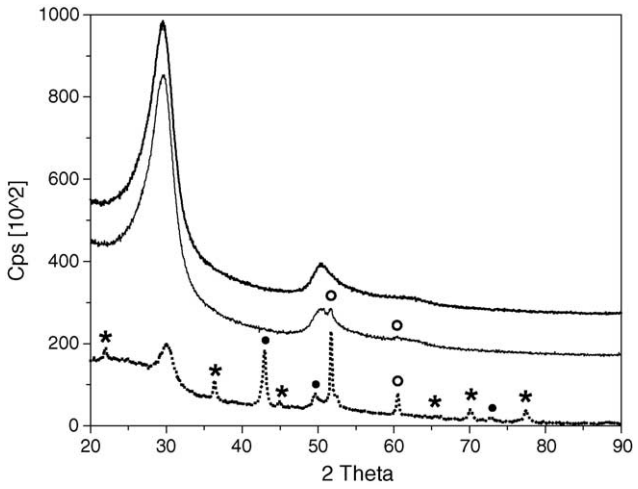

Fig. 2. XRD patterns of the Co(TMPP) precursor (dashed line), of the Co(TMPP)/Shawinigan mixture (fine line) and of the bare Shawinigan (bold line) recorded after the heat treatment under nitrogen flux; (°) Co, (●) CoO, (*) Co_3O_4.

The formation of an oxidic phase in an inert atmosphere could be related to the presence of oxygen coming from trace air in the nitrogen gas used for the TGA experiments. By increasing the temperature, the activation of oxygen takes place and oxygen atoms react with cobalt atoms. It cannot be excluded that the oxygen atoms present in the macrocycle structure could play a role, too.

The average crystallite size of the Co_3O_4 phase originated from the Co(TMPP) precursor is 29.13 nm, as determined by the Scherrer equation applied on the XRD pattern. The copresence of CoO and Co may be a result of reactions (1) and (2), as reported in Ref. [28]:

$$Co_3O_4 + H_2 \rightarrow 3CoO + H_2O \quad (1)$$

$$CoO + H_2 \rightarrow Co + H_2O \quad (2)$$

In addition to the phases mentioned above, the XRD pattern profile indicates the presence of an amorphous phase that, in our case, is due to the support employed for the measures. Finally, the intense and asymmetric peak observed at $2\theta = 30.05°$ is not correlated to the other peaks because of its broadness and shape. This peak could be tentatively ascribed to amorphous carbon coming from the thermal decomposition of the organic macrocycle, since we observed a more intense peak in the same position and with a quite similar shape in the XRD patterns of the pirolyzed bare carbon black (fine curve) and of the mixture CoTMPP/Shawinigan AB50 after thermal treatment (bold curve). Two other peaks are present in the XRD pattern of the pirolyzed mixture. These peaks, on the basis of their position (also evidenced by the difference between bold curve and fine curve, here not shown) and of the comparison with the spectrum of the pirolyzed CoTMPP (dotted curve), are related to the presence of metallic cobalt with a cubic structure.

The XRD patterns of the ex-$Co(acac)_3$ and the ex-Co(TMPP) samples recorded after the heat treatment under nitrogen flux are compared in Fig. 3, curves a and b, respectively.

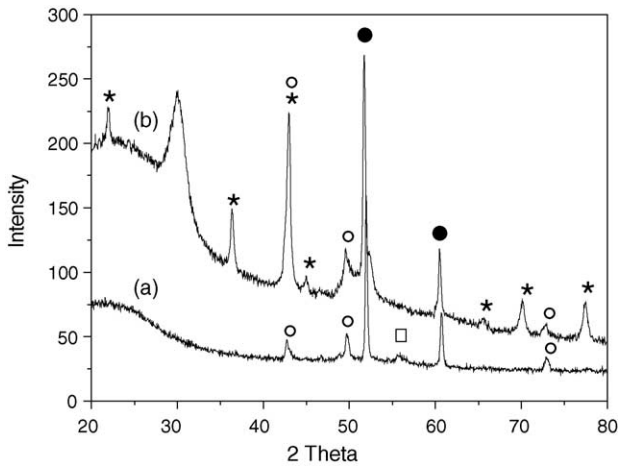

Fig. 3. Comparison between the XRD patterns of the $Co(acac)_3$ precursor (curve a) Co(TMPP) precursor (curve b) after the heat treatment under nitrogen flux; (°) CoO, (●) Co, (≤) α-Co, (*) Co_3O_4.

Mainly two distinct crystalline phases originate from the ex-$Co(acac)_3$ precursor: the CoO phase (peaks centered at $2\theta = 49.7°$ and 72.95°; JCPDS file number 9-402) and a metallic Co cubic phase ($2\theta = 60.7°$ and 51.95°; JCPDS file number 15-806). It is known that cobalt exists in two kinds of structures: hexagonal α-Co (hcp, stable at room temperature) and cubic Co (fcc, above 723 K). Mixtures of these phases normally coexist and the peak observed at $2\theta = 55.9°$ can be assigned to α-Co (JCPDS file number 5-0727). The XRD pattern profile reveals, as previously observed for the ex-CoTMPP sample, the presence of an amorphous phase that is related to the support employed for the measurements. No Co_3O_4 phase is observed after heat treatment in inhert atmosphere of the $Co(acac)_3$ precursor.

In Fig. 4, the HRTEM micrographs of as synthetized Shawinigan AB50 (section a), and of the same carbon black undergone to heat treatment in the presence of CoTMPP (section b) are reported. A concentric layer microstructure, where the particles have a globular shape, has been observed on the as prepared sample (section a). Both microstructure and morphology of the carbon black are changed after the thermal treatment at 1273 K in an inhert atmosphere in the presence of CoTMPP. The previous structure turns in a graphitic organization of the material, where the layers are easily recognizable when the carbon black is heat treated (section b).

Cobalt-containing particles have been observed by HRTEM (see Fig. 5, section a) on the heat treated CoTMPP/Shawinigan AB50 mixture. The EDS analysis (reported in section b of the same figure) was performed in two different regions of the sample that have been marked with the letters A and B. The presence of metallic cobalt (region A) and the carbonaceous nature of the layer around the particle (region B) have been evidenced. A similar morphology was already observed for heat treated tetracarboxylic

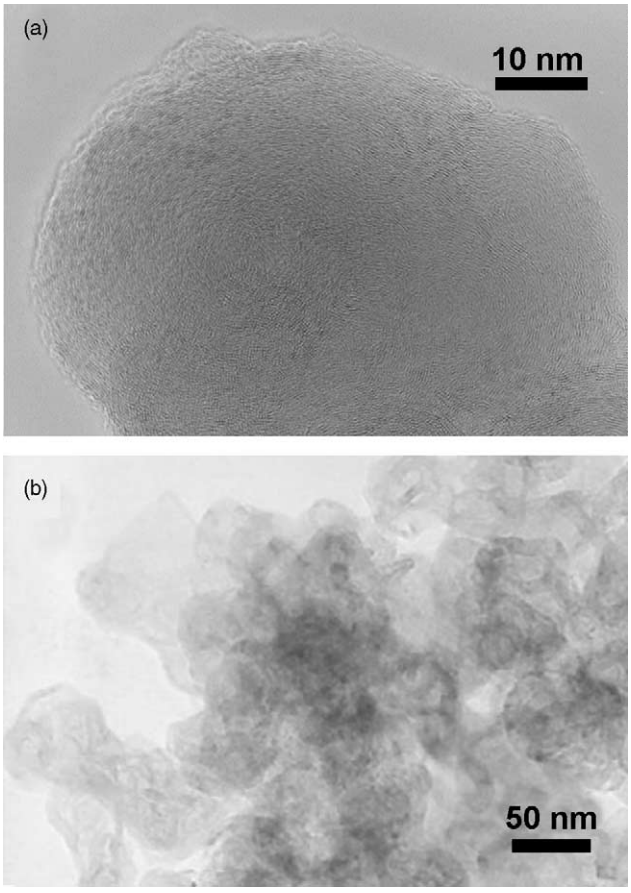

Fig. 4. HRTEM micrographs carbon black Shawinigan AB50 not undergone to heat treatment in inhert atmosphere (section a) and after the same thermal treatment in the presence of Co(TMPP) (section b). The images were taken at an original magnification of 600,000 and 100,000, respectively.

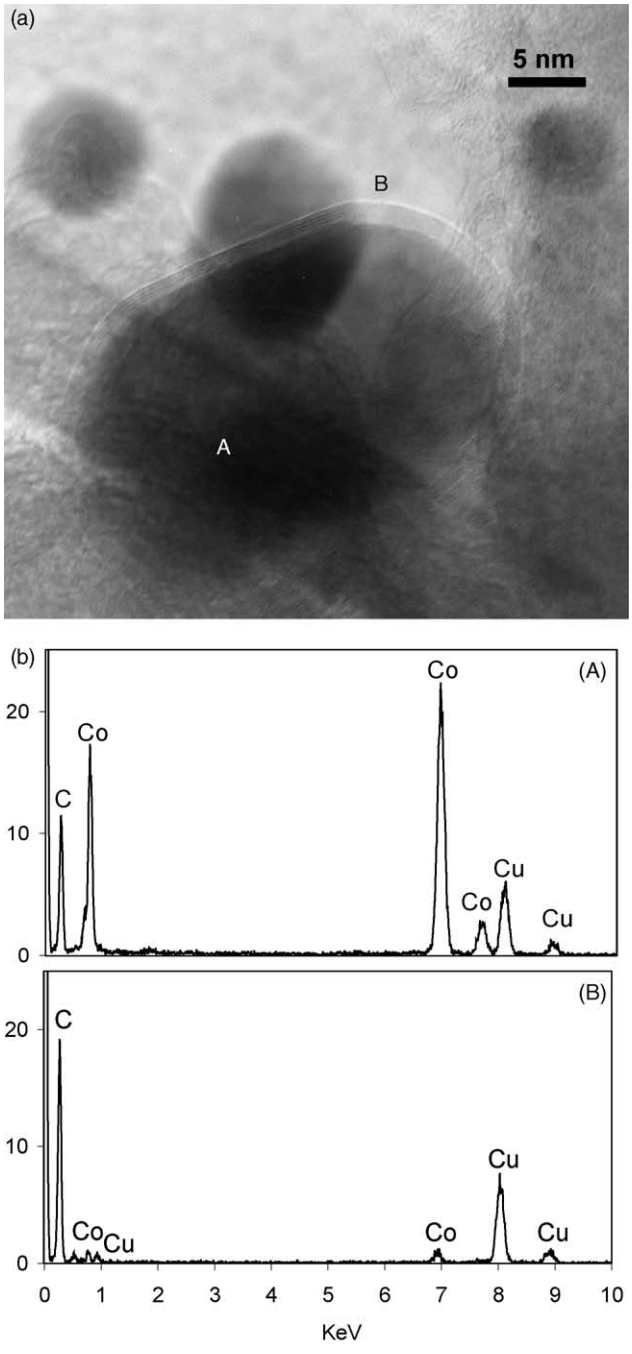

Fig. 5. HRTEM micrograph of the mixture CoTMPP/Shawinigan AB50 (section a) and EDS analysis in different regions of the same image (section b): (A) cobalt-containing particle; (B) graphitic shell around the same cobalt particle. The presence of the Cu signal in the EDS spectra is due to the grids employed for the measurements. The image was taken at an original magnification of 800,000.

cobalt phthalocyanines [21] and it is believed to be the only species responsible for the electrocatalytic activity of such Co-macrocycle/carbon black systems pyrolised at temperatures above 973 K.

Since XRD analysis of the heat treated mixture CoTMPP/Shawinigan AB50 showed that the presence of Co_3O_4 phase, we investigated by TGA the thermal decomposition of different mechanical mixtures obtained by adding to the carbon black either Co_3O_4, produced by decomposition of cobalt carbonate, or cobalt carbonate itself. The morphology of the Co_3O_4 obtained by thermal decomposition of cobalt carbonate is well illustrated in the HRTEM image reported in Fig. 6, section a. The oxide is constituted by small particles, uniform in shape and size. The mean particle size determined by the HRTEM analysis is 25 nm, being the size distribution reported in Fig. 6, section b. A value of 22 nm was found by applying the Scherrer equation to the respective XRD pattern (not shown for the sake of brevity).

Mixtures containing TMPP were also prepared. The results are reported in Fig. 7. The comparison between the weight losses of the Co_3O_4/Shawinigan AB50 mixture (solid line) and the $CoCO_3$/Shawinigan AB50 mixture (dashed line) is showed in section a. The TG curve of Co_3O_4/Shawinigan AB50 lightly decreases up to about 1023 K, then a change in slope occurs. The mixture looses the 10% of its initial weight after the thermal treatment in inhert atmosphere and almost the entire weight loss is observed above the previously mentioned temperature. In the case of $CoCO_3$/Shawinigan AB50 we calculated a total weight loss of 16.6%. Moreover, the

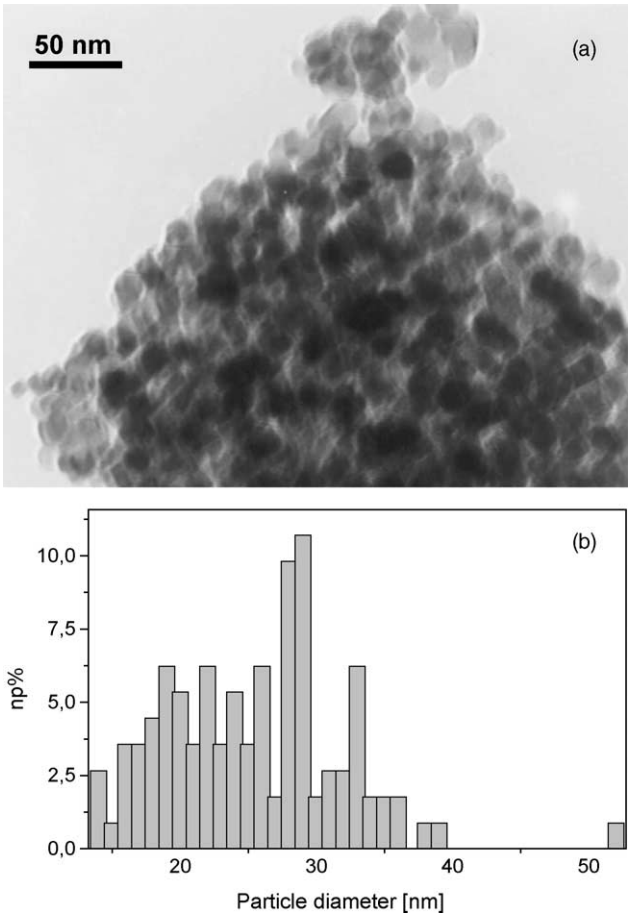

Fig. 6. HRTEM micrograph of the Co_3O_4 sample obtained from the thermal decomposition of cobalt carbonate at 673 K (section a) and particle size distribution (section b). The image was taken at an original magnification of 100,000.

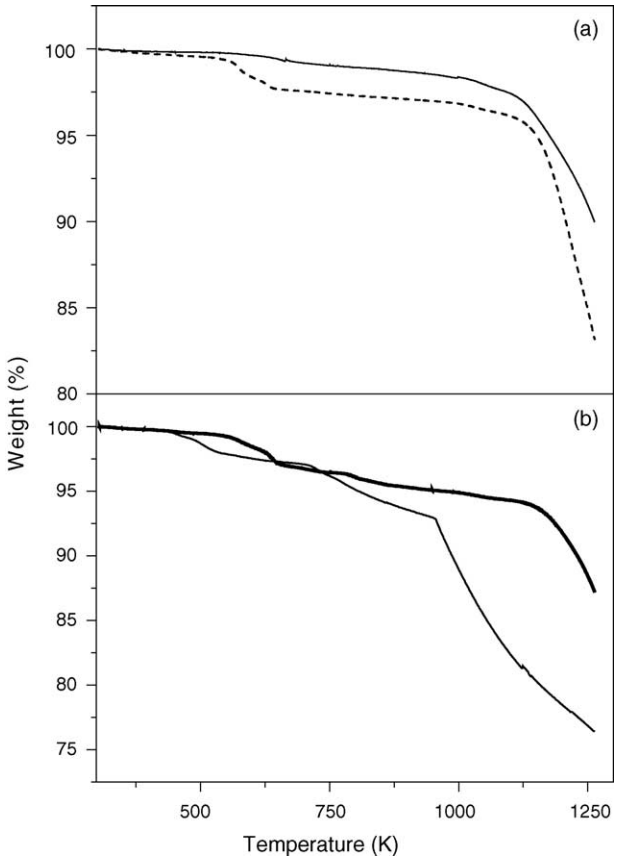

Fig. 7. Section a: TG curves related to the Co_3O_4/Shawinigan AB50 mixture (solid line) and the $CoCO_3$/Shawinigan AB50 mixture (dashed line). Section b: comparison between the TG curves of the $CoCO_3$/TMPP/Shawinigan AB50 mixture (bold line) and the CoTMPP/Shawinigan AB50 mixture (fine line). The samples were kept under a constant flux of nitrogen, using a temperature ramp of 283 K min^{-1} and starting from RT up to 1273 K.

trend is quite different because two different steps are evident in the TG curve. Two minima at 571 and at 632 K in the DTG curve, here not shown for the sake of clarity, evidence the thermal decomposition of cobalt carbonate into cobal oxide. They are associated to a weight loss of about 2%. The second step is at higher temperatures, where the majority of the weight loss takes place starting from 1065 K, similarly to what observed for the mixture containing cobalt oxide already formed. The weight losses observed in both curves at high temperature are related to some process occurring to carbon and induced by the presence of cobalt, as already observed for the mixtures containing CoTMPP and $Co(acac)_3$. Furthermore, the weight loss occurred in the case of $CoCO_3$/Shawinigan AB50 is higher than that observed for Co_3O_4/Shawinigan AB50. This could be probably due to the enhanced dispersion of the cobalt oxide, because it is synthesized during the heat treatment, since a higher dispersion of the metal guarantees an enhanced activity in the reaction catalysed by cobalt.

We performed the heat treatment on the same mixtures on which also TMPP was introduced. In both mixtures, the effect of the presence of the organic macrocycle during the heat treatment exentially results in an enhanced weight loss in the temperature range 650–1130 K (not shown for the sake of brevity), explained by the partial decomposition of TMPP. In particular, the total weight loss observed for $CoCO_3$/TMPP/Shawinigan AB50 is 12.72% (Fig. 7, bold curve in section b). It was found [18] that the catalytic activity of this pyrolised material in oxygen electroreduction is higher than that shown by the other pyrolysed mixtures following the order: $CoCO_3$/TMPP/Shawinigan AB50 $\gg$ Co_3O_4/TMPP/Shawinigan AB50 $\sim$ Co_3O_4/Shawinigan AB50, indicating that Co_3O_4 does not increase its activity in the presence of TMPP. Moreover, pyrolised $CoCO_3$/TMPP/Shawinigan AB50 showed an increase in activity also respect to CoTMPP/Shawinigan AB50, whose TG curve is reported as comparison, too (fine curve).

4. Conclusions

The Co(TMPP) precursor is more thermally stable than $Co(acac)_3$, as indicated by the TGA measurements. Moreover, XRD analysis reveals the presence of the Co_3O_4 phase

after thermal treatment in inert atmosphere, only in the case of the Co(TMPP) precursor.

The formation of tunnels or pores, induced by the presence of cobalt (as evidenced by TGA) produces an enhancement of the surface area of the active carbon and can explain the major activity of the ex-CoTMPP/carbon black system respect to the Co_3O_4/C mixture [14]. This phenomenon is particularly evident for Shawinigan AB50 and it is practically not observed in the case of Vulcan XC72R.

The HRTEM analysis showed that the Co_3O_4 particles formed in the decomposition of Co(TMPP) have very similar size respect to those of Co_3O_4 originated from the thermal decomposition of cobalt carbonate at 673 K, in spite of the significantly higher temperature treatment, but the structure of the metal macrocycle seems not to be the factor responsible for the electrocatalytic activity of the resulting material [12,17,18].

The simultaneous presence of the cobalt carbonate, of the organic macrocycle and of the active carbon during the heat treatment in inhert atmosphere produces a material on which the metal results more dispersed than in the case of the mixture containing Co_3O_4 already formed. Therefore, it is able to catalyse reactions on which pores or tunnels are produced into the carbon, thus resulting in an enhanced contact area. Moreover, cobalt metallic particles resulting from the heat treatment of CoTMPP are covered by a graphitic shell that can prevent the metal from corrosion. TGA measurements on pure CoTMPP (not shown) also revealed that the organic macrocycle is not totally decomposed, it could be possibly polymerised. Some fragments remain at the surface of the active carbon and can enhance the conductivity making easier the electron transfer to O_2. Further electrocatalytic tests on this materials are needed, but it can be potentially considered as for a future employ in fuel cells.

References

[1] E. Yeager, Electrochim. Acta 11 (1984) 1527–1537.
[2] A.J. Appleby, J. Electroanal. Chem. 357 (1993) 117–179.
[3] M. Tsionsky, O. Lev, J. Electrochem. Soc. 142 (1995) 2132–2138.
[4] T.D. Chung, F.C. Anson, J. Electroanal. Chem. 508 (2001) 115–122.
[5] K. Araki, S. Dovidauskas, H. Winnischofer, A.D.P. Alexiou, H.E. Toma, J. Electroanal. Chem. 498 (2001) 152–160.
[6] F.R. McLarnon, E.J. Cairns, J. Electrochem. Soc. 138 (1991) 645–664.
[7] M. Maja, C. Orecchia, M. Strano, P. Tosco, M. Vanni, Electrochim. Acta 46 (2000) 423–432.
[8] P. Gouérec, M. Savy, Electrochim. Acta 44 (1999) 2653–2661.
[9] L.T. Weng, P. Bertrand, G. Lalande, D. Guay, J.P. Dodelet, Appl. Surf. Sci. 84 (1995) 9–21.
[10] T. Okada, M. Yoshida, T. Hirose, K. Kasuga, T. Yu, M. Yuasa, I. Sekine, Electrochim. Acta 45 (2000) 4419–4428.
[11] G. Lalande, R. Côté, D. Guay, J.P. Dodelet, L.T. Weng, P. Bertrand, Electrochim. Acta 42 (1997) 1379–1388.
[12] A.L. Bouwkamp-Wijnoltz, W. Visscher, J.A.R. van Veen, S.C. Tang, Electrochim. Acta 45 (1999) 379–386.
[13] G. Lalande, G. Faubert, R. Côté, D. Guay, J.P. Dodelet, L.T. Weng, P. Bertrand, J. Power Sources 61 (1996) 227–237.
[14] C. Mocchi, A.C. Tavares, S. Trasatti, P. Tosco, M. Manzoli, F. Boccuzzi, in: E.W. Brooman, C.M. Doyle, C. Cominellis, J. Winnick (Eds.), Energy and Electrochemical Processes for a Cleaner Environment, vols. 2001–2003, The Electrochemical Society, Pennington, NJ, 2001, pp. 362–370.
[15] I. Nikolov, R. Darkaoui, E. Zhecheva, R. Stoyanova, N. Dimitrov, T. Vitanov, J. Electroanal. Chem. 429 (1997) 157–168.
[16] C. Bocca, G. Cerisola, E. Magnone, A. Barbucci, Int. J. Hydrogen Energy 24 (1999) 699–707.
[17] S. Gupta, D. Tryk, I. Bae, W. Aldred, E. Yeager, J. Appl. Electrochem. 19 (1989) 19–27.
[18] C. Mocchi, S. Trasatti, J. Mol. Catal. A: Chem. 204–205 (2003) 713–720.
[19] M. Watanabe, M. Tomikawa, S. Motoo, J. Electroanal. Chem. 145 (1985) 81–93.
[20] K. Tomantschger, K.V. Kordesch, J. Power Sources 25 (1989) 195–214.
[21] G. Lalande, R. Côtè, G. Tamizhmani, D. Guay, J.P. Dodelet, L. Dignard-Bailey, L.T. Weng, P. Bertrand, Electrochim. Acta 40 (1995) 2635–2646.
[22] X. Chu, L.D. Schmidt, S.G. Chen, R.T. Yang, J. Catal. 140 (1993) 543–556.
[23] Y. Tamai, H. Watanabe, A. Tomita, Carbon 15 (1977) 103–106.
[24] L.M.S. Silva, J.J.M.J.L. Figueiredo, Appl. Catal. A: Gen. 209 (2001) 145–154.
[25] R. Leboda, J. Skubiszewska-Zięba, W. Grzegorczyk, Carbon 36 (1998) 417–425.
[26] M.E. Vincett, J.A. Tsamopoulos, C.R.F. Lund, J. Catal. 126 (1990) 279–290.
[27] M.C.M. Alvim Ferraz, S. Möser, M. Tonhäeuser, Fuel 78 (1999) 1567–1573.
[28] C.-B. Wang, H.-K. Lin, C.-W. Tang, Catal. Lett. 94 (2004) 69–74.